Journal of Intelligent & Robotic Systems (2023) 108:85
https://doi.org/10.1007/s10846-023-01931-1

REGULAR PAPER

Finite-time Cooperative Guidance Law for Multiple Missiles with Impact Angle Constraints and Switching Communication Topologies

Zhiwei Hou[1] · Xuejing Lan[2] · Hongbo Chen[1] · Xuebin Zhuang[1]

Received: 28 June 2022 / Accepted: 14 July 2023

Abstract

In this paper, based on terminal sliding mode control (TSMC), a cooperative impact time and angle constrained guidance (CITACG) law for multi-missile system with switching network topologies is proposed. The obtained CITACG is composed of two parts. One part is designed to make the missiles intercept the target from their predetermined impact angles. And the other part's goal is to make the multiple missiles intercept the target simultaneously without predefining a common impact time. Sliding mode surface of the first part is designed based on TSMC, meanwhile integral terminal sliding mode control (ITSMC) and graph theory are applied to derive the second part of the CITACG. When the communication network switches between the connected topology and the disconnected one, a Lyapunov candidate function is introduced and the corresponding stability conditions are derived. The proposed guidance law is the summation of the two guidance parts, therefore it is a direct method and do not have to switch the guidance command between the impact angle constrained guidance law and the impact time constrained guidance law. The predetermined common impact time is not required in the proposed CITACG, and the missiles can automatically adjust themselves to intercept the target simultaneously by communicating between their neighbors. Numerical simulations demonstrate the great performance of the proposed guidance law.

Keywords Terminal sliding mode control · Cooperative guidance · Impact time · Impact angle · Switching topologies

1 Introduction

In recent years, multi-agent cooperative control problem has attracted researchers' significant attentions, as studied in [1, 2]. Different control methods have been applied to deal with the cooperative control problem, such as reinforcement learning method [3] and sliding mode control (SMC) [4]. The theoretical research results about multi-agent cooperative control problem were powerful tools when handling the control problem of unmanned systems, such as multi-robot system [5], multiple underwater vehicles [6] system and multiple unmanned aerial vehicles (UAVs) system. Vehicle cooperative formation strategy was one of the widely studied issues, such as in [7]. The cooperative attack strategy was another important application field of the multi-agent cooperative control method. In modernized combat, the battleships or tanks are equipped with more and more advanced self-defense systems, such as close-in weapon systems. Missiles need to penetrate the formidable defensive systems in order to destroy the target. In this case, the cooperative attack strategies can effectively enhance the lethality of the missiles. In a specific case, the salvo attack (or simultaneously attack) strategy can make the self-defense systems saturate and is an efficient cooperative attack manner.

There are two ways to achieve the goal of intercepting the target by the salvo attack of a group of cooperative multiple missiles. One way is to design the guidance law for each missile individually to achieve a common impact time. In

✉ Xuebin Zhuang
zhuangxb@mail.sysu.edu.cn

Zhiwei Hou
houzhw5@mail.sysu.edu.cn

Xuejing Lan
lanxj@gzhu.edu.cn

Hongbo Chen
chenhongbo@mail.sysu.edu.cn

[1] School of Systems Science and Engineering, Sun Yat-sen University, No. 135, Xingang Xi Road, Guangzhou 510275, People's Republic of China

[2] School of Mechanical and Electrical Engineering, Guangzhou University, 230 Wai Huan Xi Road, Guangzhou Higher Education Mega Center, Guangzhou 510006, People's Republic of China

Published online: 11 August 2023

this case, the common impact time needs to be pre-designed according to the initial conditions between the multiple missiles and the target. Then the multiple missiles can all be guided to intercept the target at the pre-designed same impact time in order to realize the salvo attack. It is not hard to see that any impact time constrained guidance (ITCG) law can be applied to achieve the salvo attack in this way. In [8], an ITCG was derived by combining the traditional proportional navigation guidance (PNG) with a feedback term of the impact time error, and the salvo attack problem was also studied. Some other control methods were also utilized to design the ITCG. Sliding mode control was applied in [9] to design the ITCG, in which the sliding mode surface was selected by introducing the impact time error. The same sliding mode surface was selected in [10], and a positive continuous nonlinear function of the lead angle was introduced to the guidance command in order to solve the singularity problem. Meanwhile, impact angle is also important in modernized combat. For instance, anti-ship or anti-tank missiles can intercept a ship or tank at a desired impact angle and destroy the weakest part of the target's armor for a more effective attack. Impact time and angle constrained guidance (ITACG) has also attracted significant attentions in recent years, as studied in [11, 12]. In [11], the traditional PNG was improved to obtain the ITACG. An additional term was designed based on the impact time error. In [12], a similar line of sight (LOS) angle rate shaping process was used, which only satisfies the impact angle constrains. Then the sliding mode surface was designed based on the desired LOS rate and the impact time error. In [13], a direct ITACG was proposed based on nonsingular terminal sliding mode control, which does not need to switch between IACG and ITCG. It's worth noting that SMC has been widely applied in the guidance and control problems of aircraft in recent years, as in [13–16].

The second way of achieving the salvo attack is homing the multiple missiles in the group cooperatively. The pre-designed common impact time is not required in this case, and the multiple missiles communicate between each other in order to synchronize the impact time. In [17], a cooperative proportional guidance, which had the same structure as PNG, was proposed. The proposed guidance law had a time-varying navigation gain which was adjusted according to the time-to-go estimation results. In [18], the cooperative guidance law was designed by combining the PNG with a cooperative control term to achieve the consensus of impact time. In [19], a three-dimensional cooperative guidance law was proposed, which had a similar structure with the guidance law presented in [18]. Considering communication delay, the problem of salvo attack guidance law design for multiple missiles against a stationary target was investigated in [20]. The distributed cooperative guidance problems for multi-missile system with time-varying delays and switching topologies were investigated in [21]. In [22], a two-step guidance strategy was proposed to realize the simultaneous attack considering the switching directed communication topologies. In [23], a finite-time distributed cooperative guidance strategies to solve the problem of the three-dimensional cooperative attacking a stationary target was investigated. Based on sliding mode control, a cooperative salvo guidance strategy using fixed finite-time consensus is proposed in [24].

Compared with the cooperative guidance law with common impact time only, less attention has been paid to the cooperative impact time and angle constrained guidance (CITACG) law for multiple missiles. In [25], a cooperative guidance law with impact time and impact angle constraints was presented. The acceleration of the missile was divided into two parts: one part was along the LOS to synchronize the impact time, and another part was perpendicular to the LOS to satisfy the impact angle constraints. The similar work for the three-dimensional guidance problem has been accomplished in [26]. In [27], without dividing the acceleration into two parts, a CITACG has been proposed. The bias PNG based guidance term was applied to achieve zero miss distance and zero impact angle error, and a cooperative control term was proposed to achieve the consensus of impact time. In [28], considering the impact time and impact angle constrains, a finite-time cooperative guidance law for multiple missiles under directed communication topologies is proposed without radial velocity measurements. In [29], two cooperative guidance schemes with impact angle and time constraints are proposed for multiple missiles system in the presence or absence of a leader missile. Taking the attitude control problem into consideration, an integrated guidance and control law was developed in [30].

In this paper, a CITACG for multi-missile system with switching communication network topologies is proposed based on the terminal sliding mode control theory. In order to satisfy the impact time and impact angle constraints simultaneously, two different sliding mode surfaces are designed, respectively. Because of the assumption that each missile has its own desired impact angle, the sliding mode surface enforcing the missile to reach the desired impact angle can be designed without using the cooperation information. While the neighbors' cooperation information of each missile is utilized when designing the sliding mode surface which synchronizes the impact time. There is not a pre-designed common impact time, and the multiple missiles communicate between each other in order to synchronize the impact time. A

Lyapunov candidate function is introduced when the communication network switches between the connected topology and the disconnected one, and the stability conditions are derived. Compared with the CITACG studied in [11–13], the proposed guidance law does not need a pre-designed common impact time. Hence, the extra design procedure of the common impact time is not required, and the missiles can on-line adjust their impact time. Because the terminal sliding mode control is applied to design the guidance law, the proposed guidance law is a finite time convergent method and has stronger robustness compared with the CITACG presented in [27]. In a real application, the communication network of the multi-missile system might be changed with time, and it might be disconnected because of the communication failure. Most of the aforementioned guidance laws have not taken it into consideration while this paper studies this problem carefully.

The main contributions of this paper are highlighted as follows: 1) Taking the switching communication network topologies into consideration, a cooperative impact time and angle constrained guidance law for multi-missile system is proposed in this paper. Compared with [21–24], the integrated cooperative impact time and angle constrained guidance problem is investigated in this paper. Compared with [28, 29], the switching communication network topologies is considered in this paper. 2) The proposed CITACG is a finite-time convergence method with strong robustness compared with [27].

The rest of the paper is organized as follows. The problem formulation is presented in Section 2. Some preliminaries are discussed in Section 3. In Section 4, the CITACG is formally proposed and the stability conditions are derived. Simulation results are presented in Section 5 to demonstrate the effectiveness of the proposed CITACG. Finally, conclusions are drawn in Section 6.

2 Problem Formulation

The two-dimensional interception problem with multiple missiles attacking one common target is described in this section. The two-dimensional guidance law is meaningful since the three-dimensional guidance problem can be decoupled into two sub-problems in the two orthogonal planes.

The engagement geometry of n missiles intercepting a common target is shown in Fig. 1. The missiles are denoted by $M_i (i = 1, \ldots, n)$ and the target is T. The velocity and the acceleration of the target are denoted by V_T and a_T, respectively. γ_T is the flight path angle of the target. Analogously, the velocity and the acceleration of the i'th missile M_i are expressed as V_{Mi} and a_{Mi}, respectively. The flight path angle of the i'th missile is γ_{Mi}. The relative distance between the i'th missile and the target is denoted by r_i and the LOS angle is θ_i. With those parameters, the kinematic engagement equations can be expressed as follows:

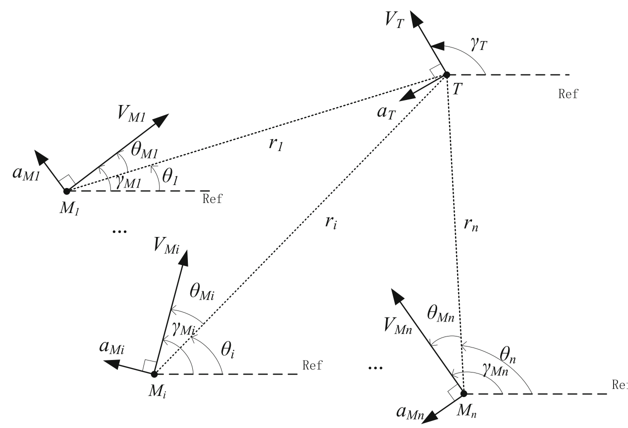

Fig. 1 Engagement Geometry

$$\begin{cases} \dot{r}_i = V_T \cos(\gamma_T - \theta_i) - V_{Mi} \cos\theta_{Mi} & i = 1, \ldots, n \\ r_i\dot{\theta}_i = V_T \sin(\gamma_T - \theta_i) - V_{Mi} \sin\theta_{Mi} & i = 1, \ldots, n \\ \dot{\gamma}_{Mi} = \frac{a_{Mi}}{V_{Mi}} & i = 1, \ldots, n \\ \dot{\gamma}_T = \frac{a_T}{V_T} \end{cases} \tag{1}$$

where

$$\theta_{Mi} = \gamma_{Mi} - \theta_i \quad i = 1, \ldots, n \tag{2}$$

Figure 2 shows the i'th missile and the target on the collision course at the time of interception. The final flight angles of the i'th missile and the target are represented as γ_{Mfi} and γ_{Tf}, respectively. The final LOS angle of the i'th missile is θ_{Fi} and the impact angle between the i'th missile and the target is denoted by θ_{impi}, which satisfies the following equation.

$$\theta_{impi} = \gamma_{Tf} - \gamma_{Mfi} \quad i = 1, \ldots, n \tag{3}$$

A further assumption is that the speed of the missile is larger than that of the target. Which means that the target-to-missile speed ratio of the i'th missile, denoted by ν_i, is less than 1.

$$\nu_i = \frac{V_T}{V_{Mi}} < 1, \quad i = 1, \ldots, n \tag{4}$$

When the i'th missile and the target are on the collision triangle, as shown in Fig. 2, the i'th missile will successfully intercept the target with zero miss-distance if the i'th missile and the target do not change their velocity anymore until the end of the interception. So the equation $r_i\dot{\theta}_i = 0$ is satisfied

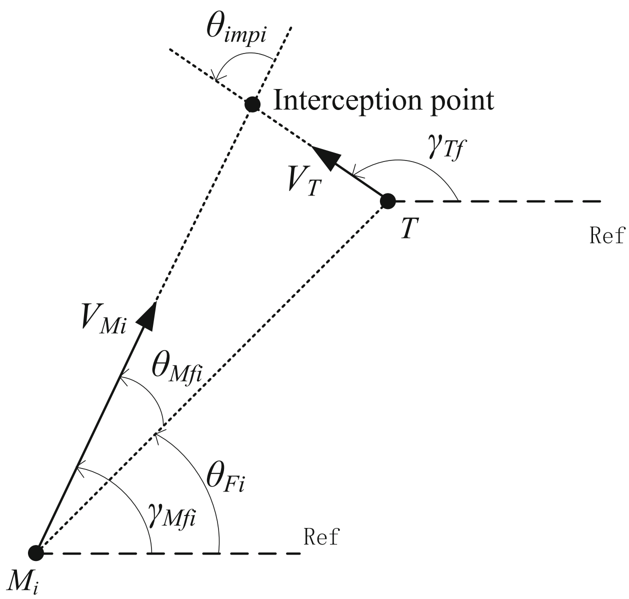

Fig. 2 Collision Course of i'th Missile and Target

and the following equation can be obtained from Eq. 1 and Fig. 2.

$$V_T \sin\left(\gamma_{Tf} - \theta_{Fi}\right) = V_{Mi} \sin\theta_{Mfi}, \quad i = 1, \ldots, n \tag{5}$$

where

$$\theta_{Mfi} = \gamma_{Mfi} - \theta_{Fi}, \quad i = 1, \ldots, n \tag{6}$$

From Eqs. 3, 4, and 5, the following relationship between the impact angle θ_{impi} and the final LOS angle θ_{Fi} of the i'th missile can be derived.

$$\theta_{Fi} = \gamma_{Tf} - \tan^{-1}\left(\frac{\sin\theta_{impi}}{\cos\theta_{impi} - \nu_i}\right), \quad i = 1, \ldots, n \tag{7}$$

With the assumption $\nu_i < 1$, it can be observed from Eq. 7 that a desired impact angle can be converted to a specific final LOS angle.

The impact time of the i'th missile t_{impi} can be defined as the following equation.

$$t_{impi} = t_{elapi} + t_{goi}, \quad i = 1, \ldots, n \tag{8}$$

where t_{elapi} is the elapsed time between the launching time of the i'th missile and the current time. And t_{goi} denotes the time-to-go, which represents the time needed by the i'th missile to intercept the target from the current time. In general, the elapsed time is a known value during the interception process while the time-to-go cannot be measured directly. So the time-to-go estimation algorithm is always required when designing the guidance laws related to the impact time.

Since the relative distance r_i, the impact angle θ_{impi} and the impact time t_{impi} are all time variant, they can be explicitly written as $r_i(t)$, $\theta_{impi}(t)$ and $t_{impi}(t)$, respectively. Where t is the current time. The following definitions are necessary in order to describe the guidance objective of the designed CITACG. The set of indices on the missiles are defined as $V \triangleq \{1, \ldots, n\}$. And the following two set are defined as:

$$V_{\min}(t) \triangleq \{i \in V : t_{impi}(t) = \min_{j \in V} t_{impj}(t)\} \tag{9}$$

$$V_{\max}(t) \triangleq \{i \in V : t_{impi}(t) = \max_{j \in V} t_{impj}(t)\} \tag{10}$$

$$\begin{aligned} &\delta(t) \triangleq t_{impi_{\max}}(t) - t_{impi_{min}}(t), \\ &i_{\max} \in V_{\max}(t), i_{\min} \in V_{\min}(t) \end{aligned} \tag{11}$$

It can be observed from Eqs. 9 and 10 that $V_{\min}(t)$ is the set of indices minimizing the corresponding impact time and $V_{\max}(t)$ is the set of indices maximizing the corresponding impact time. Equation 11 shows that $\delta(t)$ is the difference between the maximal impact time and the minimal impact time. The objectives of the designed CITACG are: 1). all missiles successfully intercept the target; 2). each missile reaches to its pre-designed impact angle; 3). all missiles intercept the target at an online-synchronized impact time. The three goals correspond to the following expressions.

$$r_i(t_f) \to 0, \quad i \in V \tag{12}$$

$$\theta_{impi}(t_f) \to \tilde{\theta}_{impi}, \quad i \in V \tag{13}$$

$$\delta(t_f) \to 0 \tag{14}$$

where t_f is the unknown impact time and $\tilde{\theta}_{impi}$ is the desired impact angle of the i'th missile.

3 Preliminaries

For the multiple missiles system studied in this paper, an undirected graph $\zeta = \{V, E\}$ is defined to describe the topology of the communication network, where $V = \{1, \ldots, n\}$ is the set of missiles and $E \subseteq \{V \times V\}$ denotes the set of edges representing all possible communication channels between the missiles. Order the (i, j) elements of E satisfying $i < j$ and assume that the graph ζ has not self-loops.

Furthermore, the topology of the communication network is assumed to be time-varying in this paper. At time instant t, the time-varying graph $\bar{\zeta}(t) = \{V, E(t), A(t)\}$ represents the instantaneous topology of the active communication network. Where $E(t) \subseteq E$ is the subset of active edges at time

t, and matrix $A(t) = \left[a_{ij}(t)\right] \in R^{n\times n}$ is the weighted adjacency matrix with $a_{ij}(t) \geq 0$. The set of neighbors of missiles i at time t is denoted by $N_i(t) = \{j \in V : (j, i) \in E(t)\}$, then the elements of matrix $A(t)$ when $k < i$ can be defined as:

$$a_{ik}(t) = \begin{cases} 1 & \text{if } k \in N_i(t) \\ 0 & \text{otherwise.} \end{cases} \tag{15}$$

Note that since the graph is assumed to be undirected without self-loops, the following relationships are satisfied.

$$a_{ki}(t) = a_{ik}(t), \quad \forall i, k \in V, \quad i \neq k \tag{16}$$

$$a_{ii}(t) = 0, \quad \forall i \tag{17}$$

4 Cooperative Guidance Law for Multiple Missiles with Switching Network Topologies

In this section, the novel CITACG is formally proposed. First the terminal impact angle constrains are considered and the IACG law is designed with a traditional method based on TSMC. Then the integrated CITACG is presented by taking the impact time into consideration. The stability conditions are analyzed when the communication network switches between the connected topology and the disconnected one. Finally, some practical improvements are shown.

Same with related works (as [13, 14, 29]), from Eq. 1, the following second-order nonlinear kinematic model can be derived.

$$\ddot{\theta}_i = -\frac{2\dot{r}_i\dot{\theta}_i}{r_i} - \frac{\cos\theta_{Mi}}{r_i}a_{Mi} + \frac{\cos(\gamma_T - \theta_i)}{r_i}a_T, \quad i \in V \tag{18}$$

This paper treats the acceleration of the target as the external disturbance and the velocity of target is considered later in the Subsection 4.3 “Practical Improvements" through the conception of predicted-intercept-point (PIP). So the basic guidance law will be designed for the stationary targets, which means $V_T = a_T = 0$. Then the kinematic model Eq. 18 can be simplified as:

$$\ddot{\theta}_i = -\frac{2\dot{r}_i\dot{\theta}_i}{r_i} - \frac{\cos\theta_{Mi}}{r_i}a_{Mi} + \Delta_i, \quad i \in V \tag{19}$$

Where Δ_i represents the model uncertainty caused by model simplification. Equation 19 shows that a_{Mi} is multiplied by $\cos\theta_{Mi}$, so that the LOS angle of i'th missile can be controlled by the i'th missile's acceleration a_{Mi} if $\cos\theta_{Mi} \neq 0$. From Fig. 1 it can be observed that the i'th missile is flying perpendicularly to the direction of the LOS when $\cos\theta_{Mi} = 0$. This state rarely occurs in real engagement scenario because that the guidance will try its best to make the missile approach the target gradually during the interception process. The point $\cos\theta_{Mi} = 0$ is not a stable equilibrium during the engagement process. So the LOS angle of i'th missile can be treated as a controllable variable. Meanwhile, we can see that θ_{impi} and ν_i in Eq. 7 are constants once the desired i'th impact angle and the i'th target-to-missile speed ratio are determined. γ_{Tf} is also a constant since the basic guidance law will be designed for the stationary target. So we can assume that the final LOS angle of the i'th missile θ_{Fi} in Eq. 7 is a constant when designing the basic guidance law.

4.1 Design of CITACG

Considering the terminal impact angle constraints, the following terminal sliding mode surface can be designed for the i'th missile based on TSMC.

$$S_{IAi} = (\theta_i - \theta_{Fi}) + \beta\left(\dot{\theta}_i - \dot{\theta}_{Fi}\right)^{\alpha}, \quad i \in V \tag{20}$$

where $\beta > 0$ and $\alpha = p/q > 0$. The parameters p and q are odd integers satisfying $1 < p/q < 2$. The Lyapunov candidate function is selected as:

$$V_{IAi} = \frac{1}{2}S_{IAi}^2, \quad i \in V \tag{21}$$

From Eqs. 20 and 21, the time derivative of the Lyapunov candidate function can be obtained as the following equation.

$$\begin{aligned}\dot{V}_{IAi} = {} & S_{IAi}[\dot{\theta}_i \\ & + \alpha\beta\dot{\theta}_i^{(\alpha-1)}(-\tfrac{2\dot{r}_i}{r_i}\dot{\theta}_i - \tfrac{\cos\theta_{Mi}}{r_i}a_{Mi} + \Delta_i)], \quad i \in V\end{aligned} \tag{22}$$

Then the IACG can be designed in the following form based on TSMC.

$$a_{IAi} = a_{IAi}^{con} + a_{IAi}^{disc}, \quad i \in V \tag{23}$$

where a_{IAi}^{con} and a_{IAi}^{disc} represent the continuous controller and the discontinuous controller respectively. They are further designed as the following forms.

$$a_{IAi}^{con} = \frac{r_i}{\cos\theta_{Mi}}\left[-\frac{2\dot{r}_i\dot{\theta}_i}{r_i} + \frac{1}{\alpha\beta}\dot{\theta}_i^{(2-\alpha)}\right], \quad i \in V \tag{24}$$

$$a_{IAi}^{disc} = \frac{\bar{M}_i}{\text{sgn}(cos\theta_{Mi})}\text{sgn}(S_{IAi}), \quad i \in V \tag{25}$$

where $\bar{M}_i$ is a constant real number needs to be selected. Let $a_{Mi} = a_{IAi}$, the following equation can be derived from Eqs.

22 and 23.

$$\dot{V}_{IAi} = -\alpha\beta\bar{M}_i\dot{\theta}_i^{(\alpha-1)}\frac{|S_{IAi}||\cos\theta_{Mi}|}{r_i} + \alpha\beta\dot{\theta}_i^{(\alpha-1)}\Delta_i S_{IAi}, \quad i \in V \tag{26}$$

According to the Lyapunov theorem, $\dot{V}_{IAi}$ should be negative definite. Therefore the stability condition can be obtained as $\bar{M}_i > \frac{|\Delta_i|r_i}{|\cos\theta_{Mi}|}$.

Then, for a given time-varying topology of the communication network $\bar{\zeta}(t) = \{V, E(t), A(t)\}$, the error of time-to-go for each missile can be defined as the following equation.

$$e_i = \sum_{j=1}^{n} a_{ij}(t_{goi} - t_{goj}), \quad i \in V \tag{27}$$

Since the real $t_{goi}, i = 1, \ldots, n$ are unknown when designing the guidance law, we let $t_{goi} \approx \hat{t}_{goi}, i = 1, \ldots, n$ where $\hat{t}_{goi}$ is the estimated time-to-go of the i'th missile. The time-to-go estimation method proposed in [31] is applied and can be expressed as:

$$\hat{t}_{goi} = \frac{r_i}{V_{Mi}}\left(1 + \frac{\theta_{Mi}^2 + \theta_{Mfi}^2}{15} - \frac{\theta_{Mi}\theta_{Mfi}}{30}\right), \quad i \in V \tag{28}$$

Then the integral terminal sliding mode surfaces are selected as:

$$S_{ITi} = e_i + \int_{t_0}^{t}\left[\frac{\bar{\alpha}}{2}e_i(\tau) + \frac{\bar{\beta}}{2^{\bar{\gamma}}}(e_i(\tau))^{\bar{\gamma}}\right]d\tau, \quad i \in V \tag{29}$$

where $\bar{\beta} > 0$, $\bar{\alpha} > 0$ and $0 < \bar{\gamma} < 1$. The current time is t and t_0 is the initial time of the engagement (usually let $t_0 = 0$).

Based on ITSMC, the CITACG proposed in this paper can be expressed in the following form.

$$a_{Mi} = a_{IAi} + a_{ITi}, \quad i \in V \tag{30}$$

Where a_{IAi} is given by Eq. 23 and a_{ITi} is an additional term which synchronizes the impact time. This additional term can be selected as:

$$a_{ITi} = a_{ITi}^{con} + a_{ITi}^{disc}, \quad i \in V \tag{31}$$

where a_{ITi}^{con} and a_{ITi}^{disc} are the continuous controller and the discontinuous controller respectively, which are designed as the following equations.

$$\begin{aligned} a_{ITi}^{con} = {} & \frac{c_i+1}{b_i} - \frac{\sum_{j=1}^{n} a_{ij}}{b_i}(-\tfrac{\bar{\alpha}}{2}e_i \\ & -\tfrac{\bar{\beta}}{2^{\bar{\gamma}}}e_i{}^{\bar{\gamma}} - \tfrac{\bar{\alpha}}{2}S_{ITi}), \quad i \in V \end{aligned} \tag{32}$$

$$a_{ITi}^{disc} = \frac{\bar{\beta}\sum_{j=1}^{n} a_{ij}}{\sqrt{2}b_i}\mathrm{sgn}(S_{ITi}), \quad i \in V \tag{33}$$

The parameters b_i and c_i are designed as the following formulations.

$$b_i = -\frac{r_i}{V_{Mi}^2}\left(\tfrac{2}{15}\theta_{Mi} - \tfrac{1}{30}\theta_{Mfi}\right), \quad i \in V \tag{34}$$

$$\begin{aligned} c_i = {} & \tfrac{r_i}{V_{Mi}}\left(\tfrac{2}{15}\theta_{Mfi}\dot{\theta}_{Mfi} - \tfrac{1}{30}\theta_{Mi}\dot{\theta}_{Mfi}\right) - \tfrac{r_i}{V_{Mi}}\left(\tfrac{2}{15}\theta_{Mi} - \tfrac{1}{30}\theta_{Mfi}\right)\dot{\theta}_i \\ & + \tfrac{\dot{r}_i}{V_{Mi}}\left(1 + \tfrac{\theta_{Mi}^2+\theta_{Mfi}^2}{15} - \tfrac{\theta_{Mi}\theta_{Mfi}}{30}\right), \quad i \in V \end{aligned} \tag{35}$$

The parameters b_i and c_i are selected in such relatively complex forms because that the time derivative of the applied time-to-go estimation method Eq. 28 is relatively complex. The detailed derivations of Eq. 36 will show how the parameters b_i and c_i are obtained.

4.2 Stability Analysis

For the convenience of elaboration, we introduce the error term about the time-to-go estimation method Eq. 28. Note that the time-to-go estimation method Eq. 28 can not precisely describe the real time to go, which means $\hat{t}_{goi} \approx t_{goi}$, $i = 1, \ldots, n$. Then from Eqs. 28, 34, and 35, the following relationship can be obtained.

$$\begin{aligned} \dot{t}_{goi} &= \dot{\hat{t}}_{goi} + \varpi_i \\ &= \tfrac{\dot{r}_i V_{Mi} - r_i\dot{V}_{Mi}}{(V_{Mi})^2}\left(1 + \tfrac{\theta_{Mi}^2+\theta_{Mfi}^2}{15} - \tfrac{\theta_{Mi}\theta_{Mfi}}{30}\right) \\ &\quad + \tfrac{r_i}{V_{Mi}}\left(\tfrac{2\theta_{Mi}\dot{\theta}_{Mi}+2\theta_{Mfi}\dot{\theta}_{Mfi}}{15} - \tfrac{\dot{\theta}_{Mi}\theta_{Mfi}+\theta_{Mi}\dot{\theta}_{Mfi}}{30}\right) + \varpi_i \\ &= \tfrac{\dot{r}_i}{V_{Mi}}\left(1 + \tfrac{\theta_{Mi}^2+\theta_{Mfi}^2}{15} - \tfrac{\theta_{Mi}\theta_{Mfi}}{30}\right) \\ &\quad + \tfrac{r_i}{V_{Mi}}\left(\tfrac{2}{15}\theta_{Mfi}\dot{\theta}_{Mfi} - \tfrac{1}{30}\theta_{Mi}\dot{\theta}_{Mfi}\right) \\ &\quad + \tfrac{r_i}{V_{Mi}}\left(\tfrac{2}{15}\theta_{Mi} - \tfrac{1}{30}\theta_{Mfi}\right)\left(\tfrac{a_{Mi}}{V_{Mi}} - \dot{\theta}_i\right) + \varpi_i \\ &= c_i - b_i a_{Mi} + \varpi_i \end{aligned}, \quad i \in V \tag{36}$$

where ϖ_i represents the error term when applying the time-to-go estimation method Eq. 28.

The boundary of ϖ_i is defined as:

$$\exists \Pi \in R^+ : \forall i \in V, |\varpi_i(t)| \leq \Pi \tag{37}$$

Furthermore, the boundary of a_{IAi} is defined as:

$$\exists \Lambda \in R^{+} : \forall i \in V, |b_i a_{IAi}| \leq \Lambda \tag{38}$$

To get the sufficient conditions for finite time stability of the proposed CITACG if the communication network is not connected all the time. The following assumption is made.

Assumption 1 (From [32]): There are positive constants ν and T_{rh} satisfying $\nu \leq T_{rh}$. During any receding horizon time interval $\eta(t) = (t, t+T_{rh})$, the communication network $\bar{\zeta}(t) = \{V, E(t), A(t)\}$ of the multi-missile system Eq. 1 is connected along a subinterval $\phi(t) \subseteq \eta(t)$, which might be a continuous subinterval or formed by the union of disjoint subintervals. Assume the overall length of the subinterval $\phi(t)$ is at least equal to ν.

Inspired by the main results of [32], the following Theorem is proposed.

Theorem 1 Assume that the communication network $\bar{\zeta}(t) = \{V, E(t), A(t)\}$ of the multi-missile system Eq. 1 satisfies Assumption 1, the proposed CITACG Eq. 30 will make the TSMC variables Eq. 20 and the ITSMC variables Eq. 29 converge to zero in finite time if the following conditions are satisfied:

$$\begin{aligned}\bar{M}_i > \sup\{&|\tfrac{c_i+1}{b_i}| + |\tfrac{\sum_{j=1}^{n} a_{ij}}{b_i}| \cdot (|\tfrac{\bar{\alpha}}{2} e_i| + |\tfrac{\bar{\alpha}}{2} S_{ITi}| \\ &+ |\tfrac{\bar{\beta}}{2^{\bar{\gamma}}} e_i{}^{\bar{\gamma}}| + |\tfrac{\bar{\beta}}{\sqrt{2}}|) + \tfrac{|\Delta_i| r_i}{|\cos\theta_{Mi}|}\}, \quad i \in V\end{aligned} \tag{39}$$

$$\bar{\beta} > \sqrt{2}((\Pi + \Lambda)\frac{T_{rh}}{\nu} + \mu^2) \tag{40}$$

where $\mu \neq 0$ is a constant, Π and Λ are the boundaries expressed by Eqs. 37 and 38. The TSMC variables Eq. 20 converge to and maintains at zero, and the following finite-time consensus condition about the ITSMC Eq. 29 is satisfied.

$$\exists K, t_r \in R^{+} : \forall t > t_r, \forall i, j \in V, \quad |t_{goi}(t) - t_{goj}(t)| \leq K \tag{41}$$

where

$$K = [2(T_{rh} - \nu) + \upsilon](\Pi + \Lambda) \tag{42}$$

$$t_r \leq \frac{T_{rh}}{2\nu\mu^2} \max_{i,j \in V \times V} |t_{goi}(0) - t_{goj}(0)| \tag{43}$$

where $\upsilon > 0$ is a positive real number.

Proof Substituting the guidance law Eq. 30) into Eq. 22 leads to:

$$\begin{aligned}\dot{V}_{IAi} &= S_{IAi}\{\alpha\beta\dot{\theta}_i^{(\alpha-1)}[-\tfrac{\cos\theta_{Mi}}{r_i}(a_{IAi}^{disc} + a_{ITi}^{con} + a_{ITi}^{disc}) + \Delta_i]\} \\ &\leq -\alpha\beta\dot{\theta}_i^{(\alpha-1)}\tfrac{|\cos\theta_{Mi}||S_{IAi}|}{r_i}[\bar{M}_i - |\tfrac{c_i+1}{b_i}| \\ &\quad -|\tfrac{\sum_{j=1}^{n} a_{ij}}{b_i}| \cdot (|\tfrac{\bar{\alpha}}{2} e_i| + |\tfrac{\bar{\alpha}}{2} S_{ITi}| \\ &\quad +|\tfrac{\bar{\beta}}{2^{\bar{\gamma}}} e_i{}^{\bar{\gamma}}| + |\tfrac{\bar{\beta}}{\sqrt{2}}|)] + \alpha\beta\dot{\theta}_i^{(\alpha-1)}\Delta_i S_{IAi}, \quad i \in V\end{aligned} \tag{44}$$

According to the Lyapunov stability theorem, $\dot{V}_{IAi}$ should be negative definite. Then from Eq. 44, the stability condition Eq. 39 can be obtained.

The stability condition Eq. 39 guarantees that $\dot{V}_{IAi}$ is negative definite and hence the condition for Lyapunov stability is satisfied, consequently, the sliding mode occurs. Once the sliding mode occurs, which means $S_{IAi} = 0$, the following equation can be obtained from Eq. 20.

$$\theta_i - \theta_{Fi} = -\beta\left(\dot{\theta}_i - \dot{\theta}_{Fi}\right)^{\alpha}, \quad i \in V \tag{45}$$

On integrating Eq. 45, the time required for the error term $\theta_i - \theta_{Fi}$ to reach 0 is $T_{ci} \geq 0$ and can be expressed as $T_{ci} = \left(\frac{p}{p-q}\right)|\theta_i(T_{si}) - \theta_{Fi}(T_{si})|^{(p-q)/p}$, where T_{si} is the time instant at which the sliding mode occurs. So the proposed guidance law Eq. 30 can make $S_{IAi} = 0$ and the kinematic model Eq. 19 converge to the equilibrium point within a finite time. This means that the desired impact angle can be achieved in a finite time by applying the proposed guidance law.

The following error variable for each edge of the communication network is defined.

$$\sigma_{ij}(t) = t_{goi}(t) - t_{goj}(t), \quad (i, j) \in E(t) \tag{46}$$

For the first-order multiple time-to-go relationship Eq. 36, consider the following Lyapunov candidate function.

$$\bar{V}_{IT} = |\sigma_{i_{\max} j_{\min}}(t)| \tag{47}$$

where

$$i_{\max} = \underset{h \in V}{\operatorname{argmax}}(t_{goh}), \quad j_{\min} = \underset{h \in V}{\operatorname{argmin}}(t_{goh}) \tag{48}$$

From Eqs. 30, 36, 46, and 47, the time derivative of the Lyapunov candidate function can be derived as Eq. 49.

$$
\begin{aligned}
&\dot{\bar{V}}_{IT} = \mathrm{SGN}(\sigma_{i_{\max} j_{\min}}(t)) \cdot \dot{\sigma}_{i_{\max} j_{\min}}(t) \\
&= \mathrm{SGN}(\sigma_{i_{\max} j_{\min}}(t)) \cdot (\dot{t}_{go i_{\max}} - \dot{t}_{go j_{\min}}) \\
&= \mathrm{SGN}(\sigma_{i_{\max} j_{\min}}(t)) \cdot (c_{i_{\max}} - b_{i_{\max}} a_{M i_{\max}} + \varpi_{i_{\max}} \\
&- c_{j_{\min}} + b_{j_{\min}} a_{M j_{\min}} - \varpi_{j_{\min}}) \\
&= \mathrm{SGN}(\sigma_{i_{\max} j_{\min}}(t)) \cdot [(\varpi_{i_{\max}} - \varpi_{j_{\min}}) + c_{i_{\max}} - b_{i_{\max}} (a_{IA i_{\max}} + a_{IT i_{\max}}) \\
&- c_{j_{\min}} + b_{j_{\min}} (a_{IA j_{\min}} + a_{IT j_{\min}})] \\
&= \mathrm{SGN}(\sigma_{i_{\max} j_{\min}}(t)) \cdot [(\varpi_{i_{\max}} - \varpi_{j_{\min}}) - (b_{i_{\max}} a_{IA i_{\max}} - b_{j_{\min}} a_{IA j_{\min}}) \\
&+ \sum_{j=1}^{n} a_{i_{\max} j} (-\tfrac{\bar{\alpha}}{2} e_{i_{\max}} - \tfrac{\bar{\beta}}{2\bar{\gamma}} (e_{i_{\max}})^{\bar{\gamma}} - \tfrac{\bar{\alpha}}{2} S_{IT i_{\max}} - \tfrac{\bar{\beta}}{\sqrt{2}} \mathrm{sgn}(S_{IT i_{\max}})) \\
&- \sum_{i=1}^{n} a_{j_{\min} i} (-\tfrac{\bar{\alpha}}{2} e_{j_{\min}} - \tfrac{\bar{\beta}}{2\bar{\gamma}} (e_{j_{\min}})^{\bar{\gamma}} - \tfrac{\bar{\alpha}}{2} S_{IT j_{\min}} - \tfrac{\bar{\beta}}{\sqrt{2}} \mathrm{sgn}(S_{IT j_{\min}}))]
\end{aligned}
\tag{49}
$$

In Eq. 49, we have:

$$
\mathrm{SGN}(\sigma_{i_{\max} j_{\min}}(t)) = \begin{cases} 1 & \text{if } \sigma_{i_{\max} j_{\min}}(t) > 0 \\ [-1, 1] & \text{if } \sigma_{i_{\max} j_{\min}}(t) = 0 \\ -1 & \text{if } \sigma_{i_{\max} j_{\min}}(t) < 0 \end{cases} \tag{50}
$$

When the connectivity property of the switching communication network is not guaranteed, according to the definition of $i_{\max}$ and $j_{\min}$, the in-equation 51 can be obtained.

$$
\begin{aligned}
&\Bigg[\sum_{j=1}^{n} a_{i_{\max} j} \left(-\tfrac{\bar{\alpha}}{2} e_{i_{\max}} - \tfrac{\bar{\beta}}{2\bar{\gamma}} (e_{i_{\max}})^{\bar{\gamma}} - \tfrac{\bar{\alpha}}{2} S_{IT i_{\max}} - \tfrac{\bar{\beta}}{\sqrt{2}} \mathrm{sgn}\left(S_{IT i_{\max}}\right)\right) \\
&- \sum_{i=1}^{n} a_{j_{\min} i} \left(-\tfrac{\bar{\alpha}}{2} e_{j_{\min}} - \tfrac{\bar{\beta}}{2\bar{\gamma}} \left(e_{j_{\min}}\right)^{\bar{\gamma}} - \tfrac{\bar{\alpha}}{2} S_{IT j_{\min}} - \tfrac{\bar{\beta}}{\sqrt{2}} \mathrm{sgn}\left(S_{IT j_{\min}}\right)\right)\Bigg] \le 0
\end{aligned}
\tag{51}
$$

From Eqs. 49 and 51, we can conclude that

$$
\dot{\bar{V}}_{IT} \le 2 \cdot (\Pi + \Lambda), \quad t \in \eta(t) \backslash \phi(t) \tag{52}
$$

This means that the Lyapunov candidate function might increase if the connectivity property of the switching communication network is not guaranteed. When the communication network is connected, it's not hard to get the following relationship according to the definition of $i_{\max}$ and $j_{\min}$.

$$
e_{i_{\max}} > 0, S_{IT i_{\max}} > 0, e_{j_{\min}} < 0, S_{IT j_{\min}} < 0 \tag{53}
$$

From Eqs. 49, 51, and 53, we can conclude that

$$
\dot{\bar{V}}_{IT} \le 2 \cdot (\Pi + \Lambda) - \sqrt{2} \cdot \bar{\beta}, \quad t \in \phi(t) \tag{54}
$$

From Assumption 1, Eqs. 52 and 54, the following relation can be obtained.

$$
\begin{aligned}
&\bar{V}_{IT}(t + T_{rh}) - \bar{V}_{IT}(t) \\
&= \int_{\phi(t)} \dot{\bar{V}}_{IT}(\tau) d\tau + \int_{\eta(t) \backslash \phi(t)} \dot{\bar{V}}_{IT}(\tau) d\tau \\
&\le \nu(2(\Pi + \Lambda) - \sqrt{2} \cdot \bar{\beta}) + (T_{rh} - \nu) 2(\Pi + \Lambda) \\
&= -\sqrt{2} \nu \bar{\beta} + 2 T_{rh} (\Pi + \Lambda)
\end{aligned}
\tag{55}
$$

By using the stability condition Eq. 40 with Eq. 55, the following condition can be derived.

$$
\bar{V}_{IT}(t + T_{rh}) - \bar{V}_{IT}(t) \le -2\nu\mu^2 \tag{56}
$$

This guarantees that there existents a finite time t_r such that $\bar{V}_{IT}(t_f) = 0$. From Eq. 56, the following relation can be derived.

$$
t_r \le \frac{T_{rh}}{2\nu\mu^2} \bar{V}_{IT}(0) \tag{57}
$$

which is equivalent with Eq. 43.

Then for any t' satisfying $\bar{V}_{IT}(t') = 0$, along the time interval $t \in (t', t' + T_{rh})$, the Lyapunov function might increase. From Assumption 1 and Eq. 52, the boundary of the Lyapunov function can be calculated as follow:

$$
\bar{V}_{IT}(t) \le [2(T_{rh} - \nu) + \upsilon](\Pi + \Lambda) \tag{58}
$$

which is equivalent with Eqs. 41 and 42. Theorem 1 is proven.

Note that the parameter t_r is a certain finite time satisfying inequality Eq. 57 (i.e. inequality Eq. 43). After t_r, the error of the cooperative impact time will maintain within a boundary K, which is represented by Eq. 42. □

4.3 Practical Improvements

In implementation, the acceleration of the missile is a finite value. When applying the proposed CITACG Eq. 30, the accelerations of the missiles can be limited through the following equations.

$$
a_{Mi} := \begin{cases} a_{M\ \max} \mathrm{sgn}(a_{Mi}) & \text{if} |a_{Mi}| \ge a_{M\ \max} \\ a_{Mi} & \text{if} |a_{Mi}| < a_{M\ \max} \end{cases}, \quad i \in V \tag{59}
$$

Because of the applying of TSMC and ITSMC, the sign function has been introduced into the CITACG as shown in the discontinuous controller parts Eqs. 25 and 33. This might cause the chattering phenomenon of the missile's accelerations. To weaken the chattering phenomenon to a certain degree, a smoothing method is utilized in this paper. When $|S_{IAi}| < \omega_{IA}$, $|S_{ITi}| < \omega_{IT}$, $i \in V$, where $\omega_{IA} > 0$, $\omega_{IT} > 0$ are two small positive real numbers, the following sigmoid functions are used to replace the sign functions $\mathrm{sgn}(S_{IAi})$ and $\mathrm{sgn}(S_{ITi})$ in the proposed CITACG, respectively.

$$\mathrm{sgmf}(S_{IAi}) = 2\left(\frac{1}{1+\exp^{-\Xi_{IA}S_{IAi}}} - \frac{1}{2}\right), \quad \Xi_{IA} > 0, \quad i \in V \tag{60}$$

$$\mathrm{sgmf}(S_{ITi}) = 2\left(\frac{1}{1+\exp^{-\Xi_{IT}S_{ITi}}} - \frac{1}{2}\right), \quad \Xi_{IT} > 0, \quad i \in V \tag{61}$$

The positive constant parameters Ξ_{IA} and Ξ_{IT} should be selected inversely proportional to ω_{IA} and ω_{IT}, respectively. By the way, to weaken the chattering phenomenon, other similar continuous functions can also be applied to replace the sign function, such as the saturation function, hyperbolic tangent function or the following simple continuous function: $\theta(s) = \frac{s}{|s|+\Delta}$, $\Delta > 0$.

In Eqs. 32 and 33, the parameter b_i might be a small number which may cause the singularity problem of the missile's acceleration. Inspired by [11], the following coefficient is introduced into the proposed CITACG.

$$\psi\left(b_i\right) = \begin{cases} 0, & |b_i| < o_1 \\ \frac{|b_i|-o_1}{o_2-o_1}, & o_1 \le |b_i| \le o_2 \\ 1, & |b_i| > o_2 \end{cases}, \quad i \in V \tag{62}$$

where $0 < o_1 < o_2$ are two small constants. Then the addition term Eq. 31 of the CITACG can be replaced by:

$$a_{ITi} = \psi\left(b_i\right)\left(a_{ITi}^{eq} + a_{ITi}^{disc}\right), \quad i \in V \tag{63}$$

By utilizing the conception of predicted-intercept-point (PIP), the proposed CITACG can be naturally extended to the engagement case when the target has a constant velocity. Figure 3 shows the engagement scene with a constant velocity instead of a stationary target. The current position of the target is indicated as (x_{t0}, y_{t0}) and the predicted-intercept-point is denoted by PIP_i, whose position is (x_{tPIPi}, y_{tPIPi}).

Utilizing the estimated time-to-go, the distance between point T and point PIP_i can be calculated as:

$$|TPIP_i| = \bar{t}_{goi} V_T \tag{64}$$

where $\bar{t}_{goi}$ is the mean value of the time-to-go estimation of the i'th missile and its neighbors, which means:

$$\bar{t}_{goi} = (\hat{t}_{goi} + \sum_{j=1}^{n} a_{ij}\hat{t}_{goj})/(1 + \sum_{j=1}^{n} a_{ij}), \quad i \in V \tag{65}$$

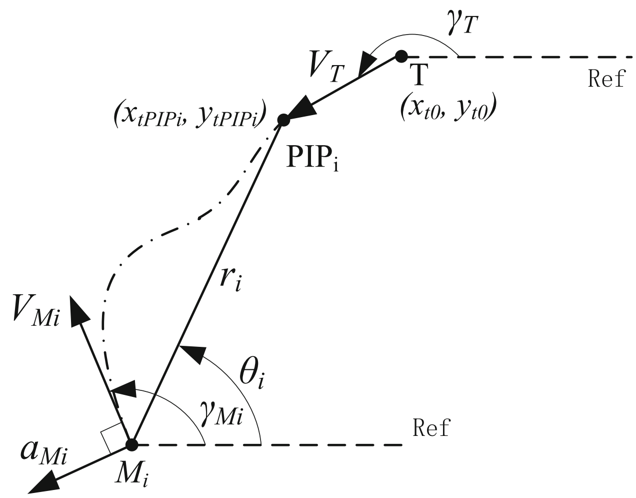

Fig. 3 PIP with Constant Velocity Target

Then the coordinates of the PIP_i's position can be calculated as:

$$\begin{cases} x_{tPIPi} = x_{t0} + |TPIP_i|\cos(\gamma_T) \\ y_{tPIPi} = y_{t0} + |TPIP_i|\sin(\gamma_T) \end{cases}, \quad i \in V \tag{66}$$

The PIP_i can be treated as the stationary target that need to be intercepted by the i'th missile. So with the application of PIP, the proposed CITACG has been naturally extended to the engagement case when the target has a constant velocity.

Note that the PIP_i might be different for different missiles because that $\bar{t}_{goi}$ are not the same for $i \in V$. But this does not affect the guidance law severely because that the time-to-go for different missiles are synchronized with time by applying the CITACG. And the PIP_is will converge to a same point within a finite time.

5 Simulation Results

In this section, several simulation results are presented to demonstrate the good performance of the proposed guidance law. First the simulation results of intercepting a stationary target cooperatively by four missiles are shown. Then the target is assumed to be maneuvering and the simulation results are presented. To demonstrate the great performance of the proposed TSMC based CITACG (TSMC-CITACG for short), the biased proportional navigation guidance based CITACG (BPNG-CITACG for short), proposed in [27], is simulated in same situations for comparison. In all simulations, the main parameters of the proposed TSMC-CITACG are selected as the same values, as shown in Table 1. The parameters p and q should be selected to form the terminal sliding mode surface, which means that p and q shoud be odd integers satisfying $1 < p/q < 2$. $\beta > 0$ is also necessary to form the terminal

Table 1 Parameters of the Guidance Law

Parameters	Value
q	7
p	9
β	5
$\bar{M}_i$	100
$\bar{\alpha}$	1
$\bar{\beta}$	1
$\bar{\gamma}$	0.5
Ξ_{IA}, Ξ_{IT}	20, 0.5
ω_{IA}, ω_{IT}	0.5, 20
o_1	0.001
o_2	0.01

sliding mode surface. $\bar{M}_i$ is the control gain of the impact angle constrained guidance part. Larger $\bar{M}_i$ can improve the control performance but might cause more serious chattering phenomenon. Similar with $\bar{M}_i$, $\bar{\beta}$ is the control gain of the impact time constrained guidance part. $\bar{\gamma}$ should be selected satisfying $0 < \bar{\gamma} < 1$, in order to form the integral terminal sliding mode surface. The positive constant parameters Ξ_{IA} and Ξ_{IT} should be selected inversely proportional to ω_{IA} and ω_{IT}, respectively. Larger Ξ_{IA}, Ξ_{IT} and smaller ω_{IA}, ω_{IT} in Eqs. 60 and 61 correspond to the functions that are closer to sgn functions, providing higher guidance accuracy but introducing more chattering phenomenon. We tend to choose Ξ_{IA} larger than Ξ_{IT} because S_{IAi} relates to miss distance directly, and the higher guidance accuracy is required. $0 < o_1 < o_2$ are two small constants.

In the numerical simulation, the normal communication topology is assumed to be connected, as shown by Fig. 4a. As Fig. 5 shows, in every receding horizon time interval (3.5 seconds), the connected communication topology Fig. 4a takes over 3 seconds. The communication topology is randomly selected from Fig. 4b-d for the rest 0.5 second.

5.1 Stationary Target

In this subsection, the simulation results of intercepting the stationary target are presented. The initial conditions and other simulation parameters of the missiles and the target are listed in Table 2.

The traditional BPNG-CITACG is used for simulation comparison. The simulation results with BPNG-CITACG are shown in Fig. 6. Figure 6a shows the flight trajectories of four missiles and Fig. 6b shows the time-to-go errors. From Fig. 6b and c, we can conclude that the traditional BPNG-CITACG can synchronize the impact time and the time-to-go errors maintain small value. Figure 6d shows that the desired impact angles can be reached. However, the final guidance precision (L_2 norm of impact angle errors) when applying the traditional BPNG-CITACG is 0.0108°, which is poorer than the proposed TSMC-CITACG.

The simulation results with the proposed TSMC-CITACG are shown in Fig. 7. From Fig. 7a, which shows the trajectories of the missiles and the parget in (X, Y) space, it can be obtained that all four missiles can intercept the target successfully from their own desired impact angle. Figure 7c shows the time-to-go estimation results of the missiles and we can conclude that the proposed TSMC-CITACG can synchronize the impact time without the pre-designed common impact time. And Fig. 7d shows that all four missiles can achieve their own desired impact angle from the different initial conditions. Note that although some efforts have been made to weaken the chattering phenomenon caused by introducing the switching communication network, the weakened chattering is still visible in Fig. 7b and d. It is hard to entirely eliminate the chattering since the communication network is switched suddenly when the communication error happens. The final guidance precision (L_2 norm of impact angle errors) when applying the proposed TSMC-CITACG is 0.000408°, which performs better than the traditional BPNG-CITACG.

5.2 Constant Velocity Target

In this subsection, the simulation results of intercepting the constant velocity target are presented. Both methods, BPNG-CITACG and TSMC-CITACG, utilize the conception of PIP. The initial conditions and other simulation parameters of the missiles and the target are listed in Table 3.

The speed of the target is 100m/s, the lateral acceleration of the target is $0.5\sin(0.1t)\mathrm{m/s}^2$ and the flight path angle γ_T is 30°. The simulation results with the traditional BPNG-CITACG are shown in Fig. 8. Figure 8a shows that four missiles intercept the target at the same time, which means the traditional method can synchronize the impact time, which can also be obtained from Fig. 8b and c. However, Fig. 8d shows that the desired impact angles can not be reached when applying the traditional BPNG-CITACG. The L_2 norm of impact angle errors when applying the traditional BPNG-CITACG is 34.17°.

The simulation results with the proposed TSMC-CITACG are shown in Fig. 9. Figure 9a shows the trajectories of the missiles and the parget in (X, Y) space and we can see that the missiles successfully intercept the target from their own desired impact angle. Figure 9b shows the time-to-go errors. Figure 9c shows that the proposed TSMC-CITACG can synchronize the impact time without the pre-designed common impact time even against the moving target. From Fig. 9d one can conclude that all four missiles can achieve their

Fig. 4 Communication Topologies

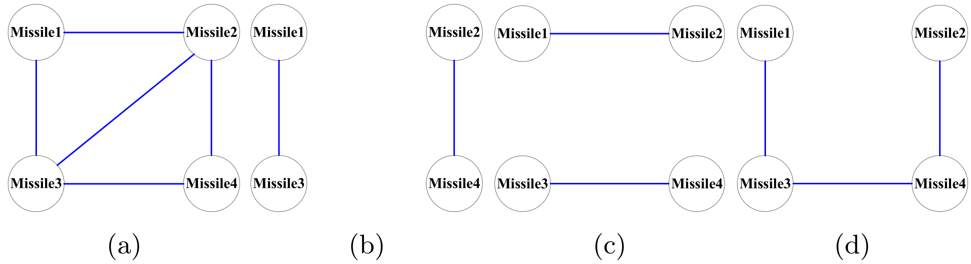

Fig. 5 Switching Communication Topologies

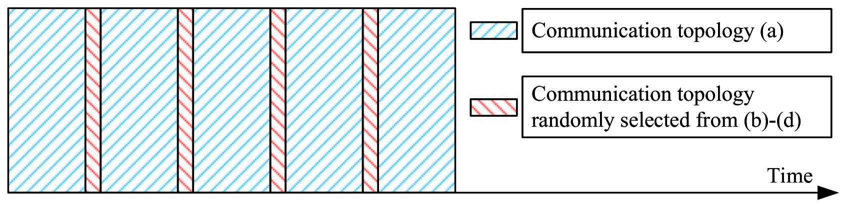

Table 2 Initial conditions and simulation parameters with stationary target

	Missile 1	Missile 2	Missile 3	Missile 4
Initial position	(−11000, 5000)m	(8000, −7000)m	(8000, −6000)m	(−5000, 10000)m
Initial flight path angle	60°	180°	90°	−60°
Speed	250m/s	250m/s	250m/s	250m/s
Desired impact angle	0°	−90°	−180°	90°
$a_{M\ \max}$	100m/s^2	100m/s^2	100m/s^2	100m/s^2

Fig. 6 Intercepting Stationary Target with Traditional BPNG-CITACG (presented in [27])

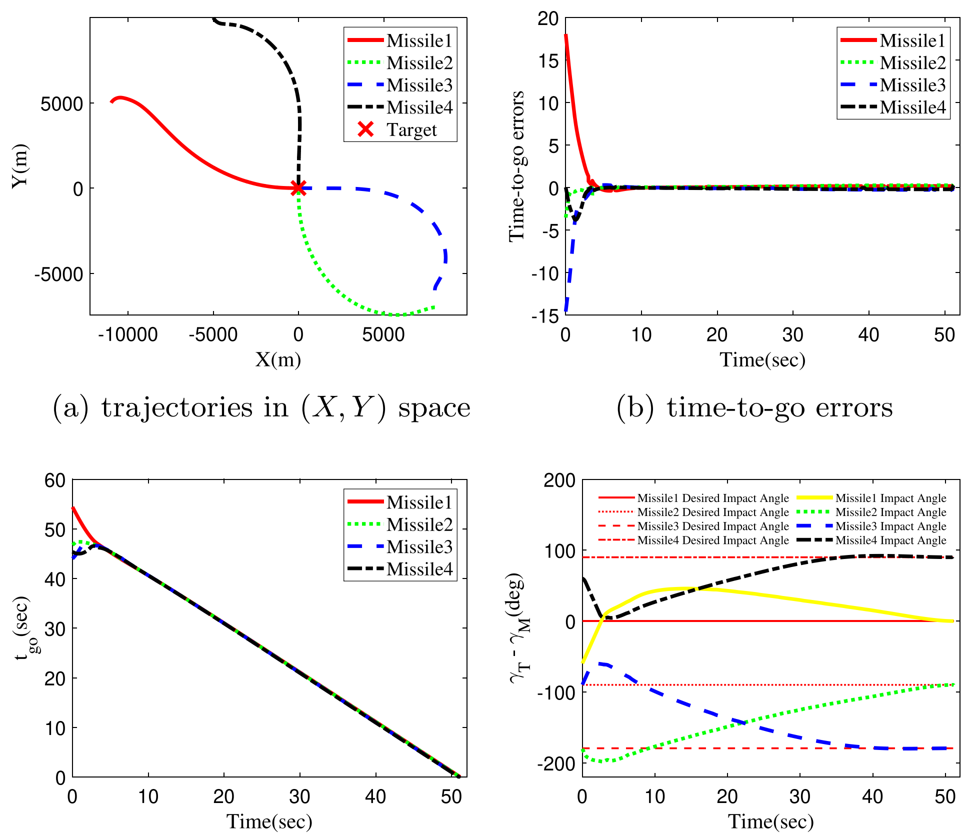

(a) trajectories in (X, Y) space (b) time-to-go errors

(c) estimated time-to-go (d) impact angles of the missiles

Fig. 7 Intercepting Stationary Target with Proposed TSMC-CITACG

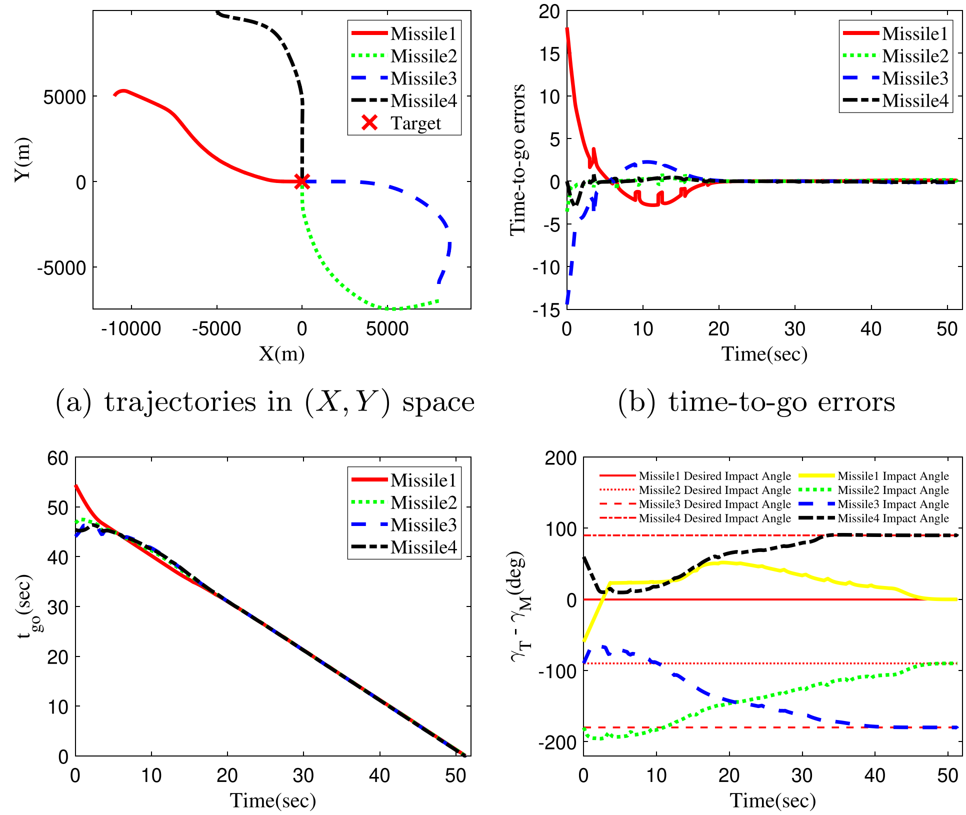

(a) trajectories in (X, Y) space (b) time-to-go errors (c) estimated time-to-go (d) impact angles of the missiles

own desired impact angle from the different initial conditions when intercepting the moving target. The L_2 norm of impact angle errors when applying the proposed TSMC-CITACG is $0.5°$. The simulation results show that the proposed TSMC-CITACG can be naturally extended to the engagement case when the target has a constant velocity by utilizing the conception of PIP.

L_2 norm of impact angle errors in two simulation cases are concluded in Table 4. It can be obtained that the proposed TSMC-CITACG improves the guidance precision compared with the traditional BPNG-CITACG, especially in the simulation case of constant velocity target.

6 Conclusion

A new cooperative impact time and angle constrained guidance law for multi-missile network with switching communication topologies is proposed in this paper. Graph theory, terminal sliding mode control and integral terminal sliding mode control are utilized to design the TSMC-CITACG. The new TSMC-CITACG is a finite time convergent guidance law with strong robustness. It works well without pre-designing the common impact time even if the connectivity property of the switching communication network is not guaranteed all the time. Based on Lyapunov theory, the stability condi-

Table 3 Initial conditions and simulation parameters with constant velocity target

	Missile 1	Missile 2	Missile 3	Missile 4
Initial position	(−8000, 8000)m	(8000, −7000)m	(11000, −7000)m	(−5000, 10000)m
Initial flight path angle	$-60°$	$180°$	$180°$	$-60°$
Speed	250m/s	250m/s	250m/s	250m/s
Desired impact angle	$30°$	$-30°$	$-60°$	$60°$
$a_{M\ \max}$	100m/s^2	100m/s^2	100m/s^2	100m/s^2

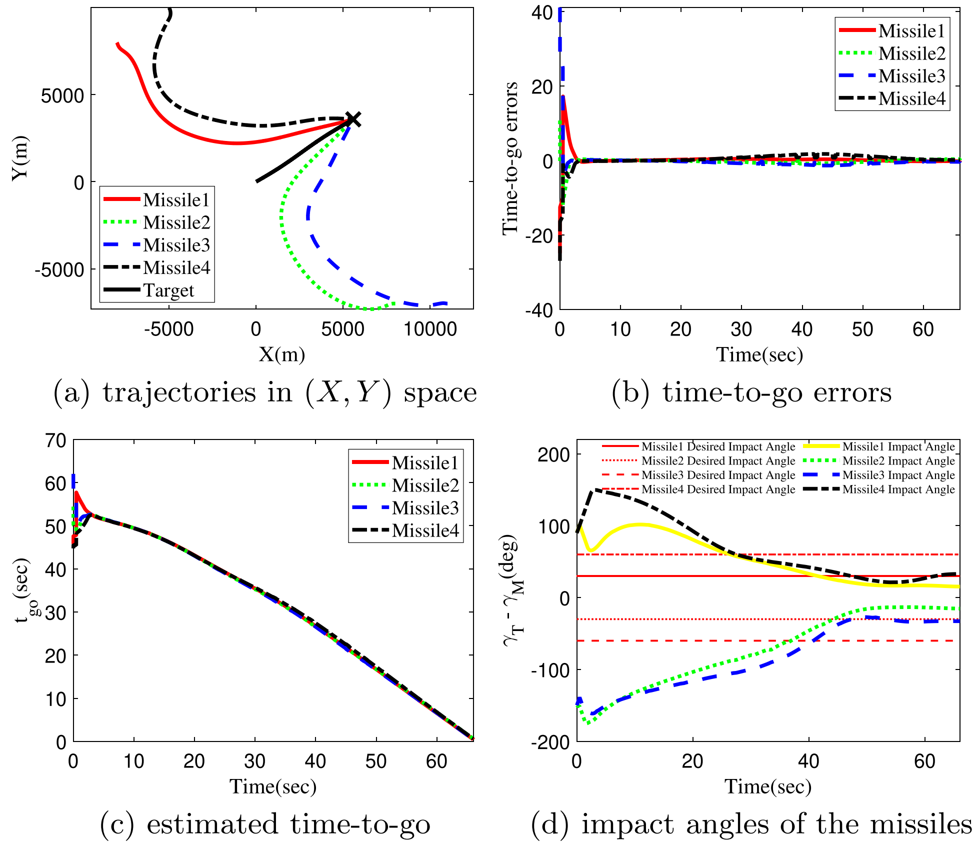

(a) trajectories in (X, Y) space (b) time-to-go errors

(c) estimated time-to-go (d) impact angles of the missiles

Fig. 8 Intercepting Constant Velocity Target with Traditional BPNG-CITACG(presented in [27])

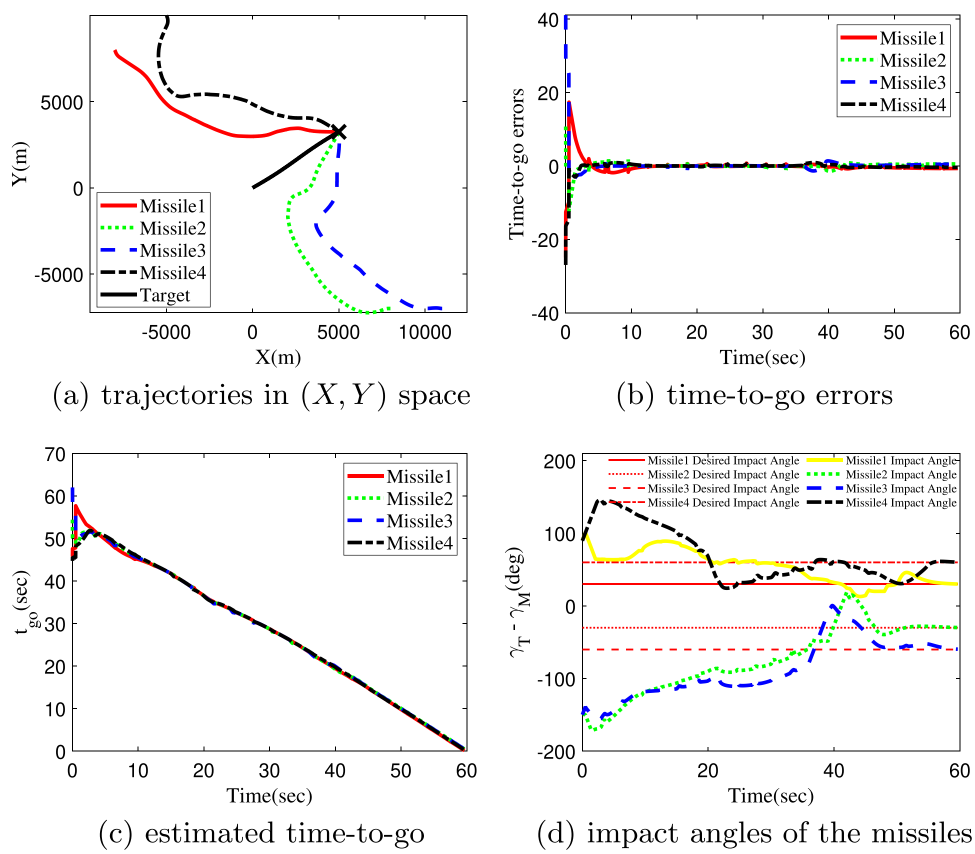

(a) trajectories in (X, Y) space (b) time-to-go errors

(c) estimated time-to-go (d) impact angles of the missiles

Fig. 9 Intercepting constant velocity target with proposed TSMC-CITACG

Table 4 L_2 norm of impact angle errors

	BPNG-CITACG (in [27])	TSMC-CITACG (proposed)
Stationary target simulation case	1.08×10^{-2}	4.08×10^{-4}
Constant velocity target simulation case	34.17	0.5

tions are analyzed and an useful theorem is presented. And the stability condition and the finite-time consensus condition are derived with the switching communication network. Finally, some practical improvements for the new TSMC-CITACG are shown. The future work focuses on designing the three-dimensional TSMC-CITACG and trying to deal with the more general communication network.

Author Contributions All authors contributed to the study conception and design. Proving, coding, experiment preparation, data collection and analysis were performed by Zhiwei Hou. The first draft of the manuscript was written by Zhiwei Hou and all authors commented on previous versions of the manuscript. All authors read and approved the final manuscript.

Funding This work is supported by the Guangdong Basic and Applied Basic Research Foundation (No. 2020A1515110815).

Data Availability The complete simulation data is available by contacting the corresponding author.

Declarations

Conflicts of interest The authors have no relevant financial or non-financial interests to disclose.

Ethics approval Not applicable. Our manuscript doesn't report the results of studies involving humans or animals.

Consent to participate Not applicable. Our manuscript doesn't report the results of studies involving humans or animals.

Consent for publication All authors have approved and consented to publish the manuscript.

References

1. Oh, K.-K., Park, M.-C., Ahn, H.-S.: A survey of multi-agent formation control. Automatica **53**, 424–440 (2015). https://doi.org/10.1016/j.automatica.2014.10.022
2. Zhang, Z., Dong, J.: Containment control of interval type-2 fuzzy multiagent systems with multiple intermittent packet dropouts and actuator failure. J. Frank. Inst **357**(10), 6096–6120 (2020). https://doi.org/10.1016/j.jfranklin.2020.04.003
3. Zhou, W., Li, J., Liu, Z., Shen, L.: Improving multi-target cooperative tracking guidance for uav swarms using multi-agent reinforcement learning. Chinese J. Aeronaut. **35**(7), 100–112 (2022). https://doi.org/10.1016/j.cja.2021.09.008
4. Sun, Y., Shi, P., Lim, C.-C.: Event-triggered sliding mode scaled consensus control for multi-agent systems. J. Frank. Inst **359**(2), 981–998 (2022). https://doi.org/10.1016/j.jfranklin.2021.12.007
5. Jin, L., Qi, Y., Luo, X., Li, S., Shang, M.: Distributed competition of multi-robot coordination under variable and switching topologies. IEEE Transactions on Automation Science and Engineering, 1–12 (2021). https://doi.org/10.1109/TASE.2021.3126385
6. Xu, Y., Li, T., Tong, S.: Event-triggered adaptive fuzzy bipartite consensus control of multiple autonomous underwater vehicles. IET Control. Theory Appl. **14**(20), 3632–3642 (2020). https://doi.org/10.1049/iet-cta.2020.0706
7. Wu, T., Wang, J., Tian, B.: Periodic event-triggered formation control for multi-uav systems with collision avoidance. Chinese J. Aeronaut. **35**(8), 193–203 (2022). https://doi.org/10.1016/j.cja.2021.10.011
8. Jeon, I.-S., Lee, J.-I., Tahk, M.-J.: Impact-time-control guidance law for anti-ship missiles. IEEE Trans Control Syst Technol. **14**(2), 260–266 (2006). https://doi.org/10.1109/TCST.2005.863655
9. Kumar, S.R., Ghose, D.: Impact time guidance for large heading errors using sliding mode control. IEEE Trans. Aerosp Electron Syst. **51**(4), 3123–3138 (2015). https://doi.org/10.1109/TAES.2015.140137
10. Cho, D., Kim, H.J., Tahk, M.-J.: Nonsingular sliding mode guidance for impact time control. J. Guid. Control Dyn. **39**(1), 61–68 (2015). https://doi.org/10.2514/1.G001167
11. Zhang, Y., Wang, X., Ma, G.: Impact time control guidance law with large impact angle constraint. Proceedings of the Institution of Mechanical Engineers, Part G. J. Aerosp. Eng. **229**(11), 2119–2131 (2015). https://doi.org/10.1177/0954410014568466
12. Yang, Z., Wang, H., Lin, D., Zang, L.: A new impact time and angle control guidance law for stationary and nonmaneuvering targets. International J Aerosp Eng 2016 (2016). https://doi.org/10.1155/2016/6136178
13. Hou, Z., Yang, Y., Liu, L., Wang, Y.: Terminal sliding mode control based impact time and angle constrained guidance. Aerosp Sci Technol **93**, 1–10 (2019). https://doi.org/10.1016/j.ast.2019.04.050
14. Hou, Z., Liu, L., Wang, Y., Huang, J., Fan, H.: Terminal impact angle constraint guidance with dual sliding surfaces and model-free target acceleration estimator. IEEE Trans. Control Sys. Technol. **25**(1), 85–100 (2016). https://doi.org/10.1109/TCST.2016.2547984
15. Zhao, Z., Li, C., Yang, J., Li, S.: Output feedback continuous terminal sliding mode guidance law for missile-target interception with autopilot dynamics. Aerosp. Sci. Technol. **86**, 256–267 (2019). https://doi.org/10.1016/j.ast.2019.01.012
16. Guo, J., Xiong, Y., Zhou, J.: A new sliding mode control design for integrated missile guidance and control system. Aerosp Sci Technol **78**, 54–61 (2018). https://doi.org/10.1016/j.ast.2018.03.042
17. Jeon, I.-S., Lee, J.-I., Tahk, M.-J.: Homing guidance law for cooperative attack of multiple missiles. J. Guid. Control Dyn. **33**(1), 275–280 (2010). https://doi.org/10.2514/1.40136
18. Zhang, Y., Wang, X., Wu, H.: A distributed cooperative guidance law for salvo attack of multiple anti-ship missiles. Chinese J Aeronaut. **28**(5), 1438–1450 (2015). https://doi.org/10.1016/j.cja.2015.08.009
19. Zhao, J., Zhou, R., Dong, Z.: Three-dimensional cooperative guidance laws against stationary and maneuvering targets. Chinese J Aeronaut. **28**(4), 1104–1120 (2015). https://doi.org/10.1016/j.cja.2015.06.003
20. He, S., Kim, M., Song, T., Lin, D.: Three-dimensional salvo attack guidance considering communication delay. Aerosp. Sci. Technol. **73**, 1–9 (2018). https://doi.org/10.1016/j.ast.2017.11.019
21. Zhou, S., Ren, J., Heng, Y., Dong, X., Li, Q.: Distributed cooperative guidance for multi-missile system with time-varying delays and switching topologies. In: 2020 39th Chinese Control Con-

ference (CCC), pp. 3464–3470 (2020). https://doi.org/10.23919/CCC50068.2020.9189290

22. Zhao, Q., Dong, X., Liang, Z., Bai, C., Chen, J., Ren, Z.: Distributed cooperative guidance for multiple missiles with fixed and switching communication topologies. Chinese J Aeronaut. **30**(4), 1570–1581 (2017). https://doi.org/10.1016/j.cja.2017.06.009
23. Yang, X., Song, S.: Three-dimensional consensus algorithm for nonsingular distributed cooperative guidance strategy. Aerosp. Sci. Technol, 106958 (2021). https://doi.org/10.1016/j.ast.2021.106958
24. Kumar, S.R., Mukherjee, D.: Cooperative salvo guidance using finite-time consensus over directed cycles. IEEE Trans. Aerosp. Electron. Sys. **56**(2), 1504–1514 (2020). https://doi.org/10.1109/TAES.2019.2934675
25. Li, B., Lin, D., Wang, H.: Finite time convergence cooperative guidance law based on graph theory. Optik **127**(21), 10180–10188 (2016). https://doi.org/10.1016/j.ijleo.2016.08.035
26. Song, J., Song, S., Xu, S.: Three-dimensional cooperative guidance law for multiple missiles with finite-time convergence. Aerosp. Sci. Technol. **67**, 193–205 (2017). https://doi.org/10.1016/j.ast.2017.04.007
27. Wang, X., Zhang, Y., Wu, H.: Distributed cooperative guidance of multiple anti-ship missiles with arbitrary impact angle constraint. Aerosp Sci Technol **46**, 299–311 (2015). https://doi.org/10.1016/j.ast.2015.08.002
28. Lyu, T., Li, C., Guo, Y., Ma, G.: Three-dimensional finite-time cooperative guidance for multiple missiles without radial velocity measurements. Chinese J Aeronaut **32**(5), 1294–1304 (2019). https://doi.org/10.1016/j.cja.2018.12.005
29. Zhang, S., Guo, Y., Liu, Z., Wang, S., Hu, X.: Finite-time cooperative guidance strategy for impact angle and time control. IEEE Trans. Aerosp. Electron. Sys. **57**(2), 806–819 (2021). https://doi.org/10.1109/TAES.2020.3037958
30. Wang, X., Zheng, Y., Lin, H.: Integrated guidance and control law for cooperative attack of multiple missiles. Aerosp. Sci. Technol. **42**, 1–11 (2015). https://doi.org/10.1016/j.ast.2014.11.018
31. Kumar, S.R., Ghose, D.: Impact time and angle control guidance. In: AIAA Guidance, Navigation, and Control Conference, p. 0616 (2015)
32. Franceschelli, M., Giua, A., Pisano, A., Usai, E.: Finite-time consensus for switching network topologies with disturbances. Nonlinear Anal. Hybrid Syst. **10**, 83–93 (2013). https://doi.org/10.1016/j.nahs.2013.06.004

Zhiwei Hou received his BS and PhD degrees from Huazhong University of Science and Technology, China, in 2013 and 2018, respectively. From 2019 to 2020 he worked at the Hong Kong Polytechnic University, Hong Kong, China, as a Research Associate. He is currently an Assistant Professor at School of Systems Science and Engineering, Sun Yat-Sen University, China. His main research interests are UAV, sliding mode control, trajectory planning, reinforcement learning, multi-agent systems, formation control, and adaptive control.

Xuejing Lan received her B.Eng. and Ph.D. degrees from Huazhong University of Science and Technology, Wuhan, China, in 2012 and 2017, respectively. She is currently an Associate Professor in the School of Mechanical and Electrical Engineering, Guangzhou University, Guangzhou, China. Her research interests include multi-agent systems, trajectory planning, cooperative control, reinforcement learning, and intelligent control.

Hongbo Chen graduated from the School of Astronautics of Harbin Institute of Technology, and obtained a Ph.D. in aircraft design and engineering. He started his career at the First Research Institute of China Aerospace Science and Technology Corporation (CASC) in 2007; in 2018, he was transferred to the School of Systems Science and Engineering, Sun Yat-Sen University. Chen Hongbo has abundant work experience in the core positions of the aerospace industry. He has been engaged in the pre-research and innovation work of major national projects for years. His innovative research and system engineering practices concentrate on the fields of aerospace transportation systems and aerospace unmanned systems.

Xuebin Zhuang received his B.E. degree from the Department of Electronic Engineering, Xiamen University, Xiamen, China, in 2006, and his Ph.D. degree from the Department of Electronic Engineering, Tsinghua University, Beijing, China, in 2011. He is currently an Associate Professor at School of Systems Science and Engineering, Sun Yat-sen University. His research interests include intelligent unmanned systems and hypersonic vehicle technology.